Workshop on Virtual Reality Interaction and Physical Simulation VRIPHYS (2015)
F. Jaillet, G. Zachmann, and F. Zara (Editors)

Evaluation of Surface Tension Models for SPH-Based Fluid Animations Using a Benchmark Test

Markus Huber[1], Stefan Reinhardt[2], Daniel Weiskopf[1], and Bernhard Eberhardt[2]

[1]VISUS, University of Stuttgart, Germany [2]Stuttgart Media University, Germany

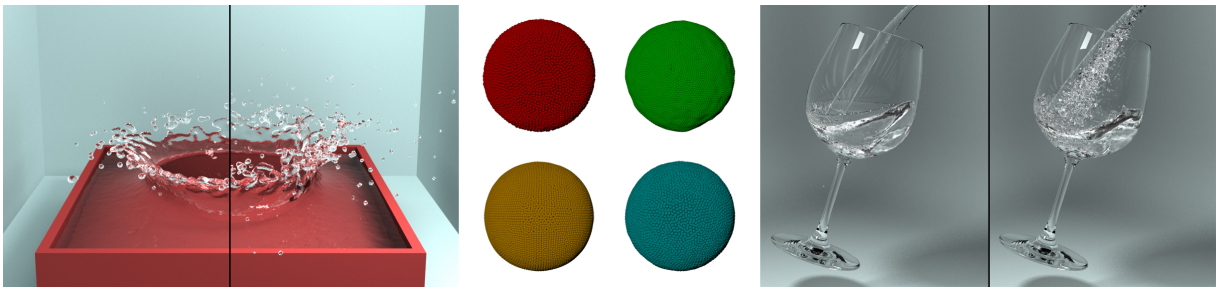

Figure 1: Different approaches to surface tension for SPH-based fluids exhibit varying characteristics. Systematic tests are performed to highlight the specific properties in three different scenarios: the development of a liquid crown (left), the formation of a spherical drop, and the pouring of liquid into a glass (right).

Abstract

We evaluate surface tension models in particle-based fluid simulation systems using smoothed particle hydrodynamics (SPH) with a benchmark test. Our benchmark consists of three experiments and a set of analysis methods that are useful for the comparison of surface tension models. Although visual quality is of major interest and is considered as well, we suggest quantification methods for the properties of these models. The goal is to identify if a certain model is suitable for a given scenario and to be able to control the results in the creation of animations. We apply the proposed evaluation methods to three existing surface tension models in combination with different SPH techniques (WCSPH, PCISPH, and IISPH) and perform systematic tests to show the influence of different settings and parameter choices. The surface tension models are chosen from different classes: a pure inter-particle force model, a model based on surface curvature, and a model using a combination of these. Additionally, we present a simple modification to improve the quality of inter-particle force models.

Categories and Subject Descriptors (according to ACM CCS): I.3.7 [Computer Graphics]: Three-Dimensional Graphics and Realism—Animation

1. Introduction

The animation of fluids for computer graphics applications using particle-based methods has gained increased attention in the last decade. Much progress in simulation methods has been achieved that allow high particle counts, complex interactions with other objects, and the representation of a wide range of materials. For liquids, surface tension is a distinctive characteristic and its effects have been identified as one of the key components to recreate physically plausible and visually appealing fluid phenomena. For fluid simulation systems based on smoothed particle hydrodynamics (SPH), several models to incorporate surface tension have already been proposed. They address the representation of the diverse effects of surface tension and the specific challenges that occur at free surfaces of particle-based fluids. These methods use different approaches to model surface tension and therefore show varying properties in their behavior and

DOI: 10.2312/vriphys.20151333

usage. Although some comparisons with other models are conducted in the original papers of the surface tension models, there are no explicit common standards for comparison that allow thorough comparative analysis. In this work, we perform a systematic evaluation of surface tension models in combination with different SPH methods using a benchmark test that is intended as a useful tool for the comparison of such models.

In computer graphics, fluids are usually modeled as single-phase free surface flow. There has been much attention and improvement in the last few years, especially regarding incompressible fluids [IOS*14]. In case of liquids, the shape of the fluid, especially at the interface of the liquid and the gas phase (e.g. water and air), is highly influenced by surface tension. Depending on the magnitude of the surface tension, various effects regarding the appearance and behavior of a liquid can be observed. Especially for single-phase fluids, there exist numerous challenges that arise with the modeling of surface tension in SPH-based fluid simulations, such as the underestimation of density at interfaces, large surface tension coefficients, and the handling of thin features. Existing techniques present a number of different approaches to overcome these difficulties: For instance, surface tension can be modeled through forces acting on the surface particles in order to minimize the curvature and hence, its energy [MCG03], [HWZ*14]. A second approach is to use cohesion forces between neighboring particles [BT07] or a combination of both techniques [AAT13]. In this work, we evaluate surface tension models with particular attention to the combination with different SPH solvers.

The variety of surface tension models in combination with the different SPH approaches makes it difficult to compare the models in detail and to determine a model's suitability for a certain task. Therefore, we intend to establish a benchmark test for the evaluation and comparability of surface tension models. We choose three SPH methods and three surface tension models as representatives for a class of techniques in each case that are outlined in Sec. 3. For the evaluation, we apply the benchmark test to existing models for the evaluation of such models. We aim to identify strengths and weaknesses of these models and understand their suitability for possible applications. The goal is to highlight key properties of surface tension models considered to create the desired animations and to facilitate the development of novel methods.

The overall contribution of this paper is the systematic evaluation of surface tension models using a benchmark test in order to determine the properties of a model not only visually, but also in a quantitative manner. The goal is to characterize surface tension models, so it is possible to improve and speed up the goal-oriented creation of fluid animations with surface tension, or to facilitate the development of novel or refined models. The specific contributions of this paper are:

- We present a benchmark test for the evaluation of surface tension models. We establish an evaluation procedure that consists of diverse scenarios, parameter testing, and interplay with different simulation systems based on SPH.
- The process is applied to three existing surface tension models in combination with three up-to-date simulation systems. For comparability and reproducibility, we use uniform settings for each of the scenarios and provide complete information, such as kernels and parameters.
- We show how a simple modification improves the quality of the surface tension model proposed by Becker and Teschner [BT07].
- We present our observations from the application of the benchmark to the surface tension models, discuss the properties of these models and how the results can be of use in the process of creating animations.

The source code of our implementation used for our evaluations is made available to the public along with example initialization files for the benchmark scenes at `http://go.visus.uni-stuttgart.de/sphevaluation`.

2. Related Work

Particle-based fluid animation has evolved to an important research area in computer graphics. Robust simulation methods and techniques for manifold effects have been developed [IOS*14]. When new techniques are presented, it is common practice to apply them to a certain set of scenarios, e.g., a breaking dam or a fluid pillar for general fluid simulation techniques, different fixed or moving obstacles for boundary handling methods, and interaction with other dynamic objects for two-way coupling models. In case of surface tension, the formation of a drop in absence of gravity and the dynamics of a liquid crown have been commonly used. Although these tests can be considered as standard procedures, they are rarely performed with uniform setups, e.g. regarding simulation methods, particle counts, and parameter values. Different configurations and sometimes missing specifications make it difficult to do a comparative evaluation and regard these scenarios universal benchmark tests.

A typical benchmark in the field of level-set methods is the rotating Zalesak disk or sphere, used to determine the quality of methods for animated surfaces (e.g. [EFFM02], [BGB15]). Using this benchmark, evaluation and especially quantification is possible, e.g. by measuring volume loss. However, to the best of our knowledge, there are no common benchmarks in fluid animation for computer graphics.

Focusing on liquids, different methods for the surface creation from the simulation particles have been proposed. The main challenge is to produce smooth surfaces that preserve the features of the fluid as accurately as possible. Zhu and Bridson [ZB05] introduce a distance-field-based method to generate smooth surfaces that is further improved by Adams et al. [APKG07] and Solenthaler et al. [SSP07]. Based on this approach, Akinci et al. [AAIT12] present a fast and

memory efficient reconstruction system with comparable results. To improve the surface quality at locations with a low particle density, Yu and Turk [YT13] use anisotropic kernels for the density field creation. Bhattacharya et al. [BGB15] use energy minimization on a level-set surface for smooth results. Also based on the approach by Zhu and Bridson [ZB05], Huber et al. [HEW15] show a method to generate surfaces at complex boundaries.

A thorough overview of current simulation methods based on SPH for computer graphics applications can be found in the recent state of the art report by Ihmsen et al. [IOS*14]. In the following section, we will present the considered SPH models and give a short description of surface tension models that are evaluated in this paper.

3. Simulation Models

As stated in Sec. 1, we perform our evaluation on combinations of different SPH solvers with surface tension models. In this section, a short overview of the used models is given.

3.1. SPH-Based Fluid Simulation

The motion of a fluid is governed by the well-known Navier-Stokes equations. For particle-based simulations, the quantities of the fluid move with particles and the Navier-Stokes equations can be expressed in the Lagrangian viewpoint as

$$\rho_i \frac{\mathrm{d}\mathbf{v}_i}{\mathrm{d}t} = -\nabla p_i + \nu\nabla^2\mathbf{v}_i + \mathbf{F}_i^b, \tag{1}$$

where $\frac{\mathrm{d}\mathbf{v}_i}{\mathrm{d}t}$ is the material derivative of a particle's velocity. In Eq. 1, ρ_i is the particle's density, $\mathbf{v}_i$ its velocity, p_i its pressure, and $\mathbf{x}_i$ its position. ν is the viscosity coefficient and $\mathbf{F}_i^b$ are the body forces acting on the particle, such as gravity.

In order to obtain a numerical solution for the motion of the particles, fluid quantities can be evaluated using the SPH method. For an elaborate overview of the established methods for the simulation of fluids with SPH, we refer the reader to the state of the art report by Ihmsen et al. [IOS*14]. As shown in their report, the common SPH methods in computer graphics mainly differ in the calculation of pressure forces. The methods can be classified by the approach of incompressibility, if it is based on an equation of state (EOS) or based on a pressure Poisson equation (PPE). In this work, we incorporate three models, each representing one class that is common in literature [IOS*14]: For a non-iterative EOS solver, we implemented the weakly compressible SPH (WCSPH) method [BT07]. The predictive-corrective incompressible SPH (PCISPH) method [SP09] is used as a representative for iterative EOS solvers with splitting, and implicit incompressible SPH (IISPH) [ICS*14] is implemented for the pressure computation based on a PPE. We choose WCSPH due to its straightforward implementation and its reasonable results and because it is used in many existing simulation systems. With PCISPH, an easy to implement incompressible fluid simulation has been presented that has been widely used in SPH-related papers. IISPH is the most recent incompressible approach and the authors have shown that it is especially suitable and efficient with large time steps and therefore, specifically useful for high particle counts.

3.2. Including Surface Tension

In this section, we briefly introduce the surface tension models used here in combination with the aforementioned simulation systems.

By now, several approaches to model surface tension with single-phase particle-based fluids have been presented. Surface tension in general can be seen from different viewpoints, either as (molecular) interaction between particles or in terms of energy that causes particles located at the interface to a (virtual) second phase to form a curvature-minimizing surface. Current surface tension approaches differ by their viewpoint and are modeled according to one viewpoint, or as a combination of these. However, they have in common that they result in forces that are integrated in Eq. 1 either as additional inter-particle forces or body forces.

In the following, we briefly summarize four surface tension models that are considered in this study. A most recent representative model for each class is chosen and a modification for the inter-particle based model is proposed. We apply the common notation with per particle quantities mass m_i, density ρ_i, and volume fraction V_i. Further, we use the abbreviation for the SPH kernel expression $W_{ij} = W(\mathbf{x}_i - \mathbf{x}_j, h)$ with the kernel smoothing length h. W_{ij}^{st} stands for the kernel used for the evaluation of surface tension.

3.2.1. Inter-Particle Interaction Forces

Becker and Teschner [BT07] propose a microscopic model for surface tension based on the work of Tartakovsky and Meakin [TM05]. In this model, the fluid particles act as actual particles with the surface tension being modeled as (molecular) forces between neighboring particles. This type of models are often referred to as inter-particle interaction forces (IIF). According to Becker and Teschner [BT07], surface tension emerges from cohesion forces between particles and results in velocities

$$\frac{\mathrm{d}\mathbf{v}_i}{\mathrm{d}t} = -\frac{\varphi}{m_i}\sum_j m_j(\mathbf{x}_i - \mathbf{x}_j)W_{ij}^{st}, \tag{2}$$

that are added to the present velocities of the particles, where φ controls the magnitude of the surface tension force. For a consistent formulation in this section and improved comparability, the surface tension model in Eq. 2 can be rewritten in terms of forces as

$$\mathbf{F}_i^{st} = -\varphi\sum_j m_j(\mathbf{x}_i - \mathbf{x}_j)W_{ij}^{st}. \tag{3}$$

3.2.2. Combined Inter-Particle and Surface Forces

Since IIF can only reproduce a portion of surface tension effects, Akinci et al. [AAT13] use a combination of inter-particle forces and forces based on surface curvature. First, the inter-particle interaction forces are modeled with a cohesion force

$$\mathbf{F}_i^{cohesion} = -\gamma m_i \sum_j m_j C(|\mathbf{x}_i - \mathbf{x}_j|) \frac{\mathbf{x}_i - \mathbf{x}_j}{|\mathbf{x}_i - \mathbf{x}_j|}. \quad (4)$$

In this force calculation, the usually used SPH kernel is replaced with a function C that includes a repulsion term for close particles similar to Tartakovski and Meakin [TM05], which is not modeled by the approach of Becker and Teschner [BT07] to avoid particle clustering. The function C is given by

$$C(r) = \frac{32}{\pi h^9} \begin{cases} (h-r)^3 r^3 & 2r > h \wedge r \leq h \\ 2(h-r)^3 r^3 - \frac{h^6}{64} & r > 0 \wedge 2r \leq h \\ 0 & \text{otherwise} \end{cases}. \quad (5)$$

In addition to the inter-particle forces, a continuum surface force (CSF) is also employed in this model [BKZ92], [MCG03]. With the CSF approach, surface tension is modeled as a pressure on the interface between the liquid and the gas phase resulting in a normal force. In contrast to Müller et al. [MCG03], the surface curvature is not calculated explicitly and the normal approximation is evaluated based on the gradient of the density field

$$\mathbf{n}_i = h \sum_j \frac{m_j}{\rho_j} \nabla W_{ij} \quad (6)$$

with a scaling factor h. Using h, normals can be calculated independent from the simulation scale. The curvature of the surface is given implicitly by the magnitude of $\mathbf{n}$ and the curvature-based force is given by

$$\mathbf{F}_i^{curvature} = -\gamma m_i \sum_j (\mathbf{n}_i - \mathbf{n}_j). \quad (7)$$

The combined surface tension force is obtained by adding the cohesion and the curvature based force as

$$\mathbf{F}_i^{st} = K_{ij}(\mathbf{F}_i^{cohesion} + \mathbf{F}_i^{curvature}), \quad (8)$$

where

$$K_{ij} = \frac{2\rho_0}{\rho_i + \rho_j} \quad (9)$$

is a symmetrized correction factor to account for particle deficiencies, e.g. in case of isolated particles or thin features.

3.2.3. Surface Forces

Recently, He et al. [HWZ*14] have presented a surface tension model that is solely based on surface energy minimization that is specifically suitable to handle thin features. Similar to CSF models [Mor00], [MCG03], it is based on a color field c that is used to distinguish regions covered by the fluid from others. Usually, c is set to 1 at the fluid particles and 0 everywhere else. With most approaches, the color field is smoothed:

$$c_i^s = \sum_j \frac{m_j}{\rho_j} c_i W_{ij}. \quad (10)$$

In contrast to the approaches by Müller et al. [MCG03] and Akinci et al. [AAT13], He et al. use the normalized term

$$\nabla c_i^s = \frac{\sum_j V_j c_j \nabla W_{ij}}{\sum_j V_j W_{ij}} \quad (11)$$

for the color field gradient to account for particle density underestimation, where V_j is the volume of particle j. Using the surface tension energy density $\frac{\kappa}{2}|\nabla c_i^s|^2$, the momentum-conserving surface tension force can be calculated by averaging the energy densities:

$$\mathbf{F}_i^{st} = \frac{\kappa}{2} \sum_i V_i V_j \left(\frac{|\nabla c_i|^2 + |\nabla c_j|^2}{2} \right) \nabla W_{ij}^{st}. \quad (12)$$

In their work, He et al. [HWZ*14] also introduce additional air pressure forces without using ghost particles which is not considered in this paper.

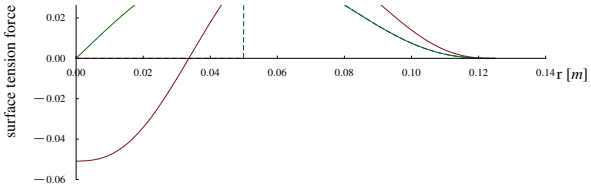

Figure 2: Different models of cohesive forces with smoothing length $h = 0.125\ s$. The model by Akinci et al. [AAT13] (red) includes repulsive forces. The model by Becker and Teschner [BT07] (green) can be modified (blue dashed) by cutting off forces to avoid particle clustering.

3.2.4. Modifications to Inter-Particle Interaction Forces

The IIF model of Becker and Teschner [BT07] is an attractive choice because of its efficiency, simplicity, and easy implementation. With this model however, it is possible that particles group in clusters because attractive forces persist with decreasing distance between particles (see Fig. 2). As it can be seen in this figure, the cohesion forces of the model by Akinci et al. [AAT13] eliminate this effect because the forces are modeled as repelling as the distance decreases. If the general model of Becker and Teschner is still preferred, one approach is to cut the cohesive forces at a certain distance to alleviate the problem of particle clustering (see Fig. 2). In addition, it is possible to remodel the cohesive force via a modified kernel function to obtain also repelling forces similar to Akinci et al.

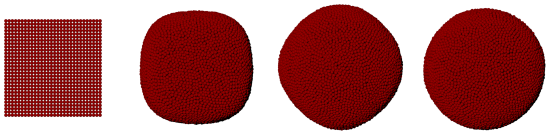

Figure 3: Snapshots of an example sequence of benchmark test 1 (Sec. 5.1). Starting from an initial cubic arrangement of particles (left), a spherical drop (right) is formed. In this case, the surface tension model by Akinci et al. [AAT13] with $\gamma = 1.0$ is used in combination with IISPH.

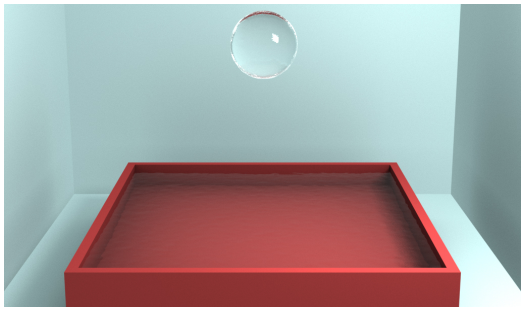

Figure 4: Initial setup of benchmark test 2 (Sec. 5.2): a spherical drop is placed over a container of liquid.

4. Implementation

As mentioned above, we incorporate WCSPH, PCISPH, and IISPH for the simulation of fluids. If not stated otherwise, we use the SPH kernel as proposed in the work of Müller et al. [MCG03], also for surface tension calculations. In all simulation systems, negative pressure values are clipped to avoid attracting pressure forces. Viscosity forces are evaluated with the SPH approximation as given in [MFZ97] and [IOS*14]. As proposed by Akinci et al. [AAT13], viscosity forces are multiplied with the correction term in Eq. 9 to account for particle deficiencies.

For WCSPH, pressure is calculated using the equation of state (EOS) as given by Becker et al. [BT07]. The pressure constant k is evaluated according to Monaghan [Mon05] using $k = |\mathbf{v}|/\eta$ allowing a maximum velocity of $|\mathbf{v}| = 100\frac{m}{s}$ and a density fluctuation of $\eta = 0.01$. For both iterative incompressible solvers (PCISPH and IISPH), we allow a maximal compression of 1%.

Boundaries, such as container walls or the glass in benchmark test 3 (Sec. 5.3), are sampled with particles and the boundary handling method by Akinci et al. [AIA*12] is employed.

For the renderings, we use the level-set technique by Bhattacharya et al. [BGB15] to extract the surface for the liquid animations.

5. Benchmark Test for Surface Tension Models

In this section, we specify the setup of our proposed benchmark test in detail. The test consists of three typical scenarios that cover settings with high curvature on relatively small surface areas, as well as larger free surfaces.

5.1. Test 1: Drop Formation

In the first scenario, $27k$ particles are initially arranged in a cube ($30 \times 30 \times 30$ particles) as shown in Fig. 3 (left) and there are no forces acting, including gravity. Upon simulation start, the particles should retain a spherically drop form due to surface tension (Fig. 3, right). Generally, surface tension forces act to minimize the surface area toward the inside of the sphere. Inside the liquid, pressure forces counteract against these forces until a equilibrium state is reached. This scenario is especially suited to closely observe the interplay between the different types of forces, as there are no external forces present and no interactions with other objects occur that would require explicit boundary handling.

For this scenario, the particle size is set to $0.025\ m$ and the particles are initially arranged with a distance of $0.05\ m$. We set $h = 0.125\ m$, a low viscosity coefficient of $\nu = 0.01$, and the simulation step size is $dt = 0.001\ s$.

For the evaluation of the properties of surface tension models, the process of drop formation is analyzed. Besides visual inspection of the animation sequences, average particle velocities, surface tension forces, and pressure forces are measured each time step. Absolute values and their change over time of these important quantities are further analyzed.

5.2. Test 2: Liquid Crown

For this second test, the spherical drop as obtained from the first test with $27k$ particles is initially placed over a container of liquid consisting of 634980 particles. In a preprocessing step, the drop as well as the liquid in the container have been simulated until a equilibrium state was achieved. Under the influence of gravity, the drop falls into the liquid, and a liquid crown will develop on impact. Surface tension influences the shape of the crown and the thin features and smaller droplets that dissolve. The parameters for this scenario are $h = 0.1\ m$, $\nu = 0.01$, and $dt = 0.001\ s$.

In this case, average particle velocities are measured for the analysis of properties of the different surface tension models in a highly dynamic scenario.

5.3. Test 3: Water Glass

In the third scenario, a liquid consisting of $400k$ particles is poured into a glass sampled with $200k$ particles as an example of a highly dynamic scene with a complex interaction object in a practical application. The particles are initially

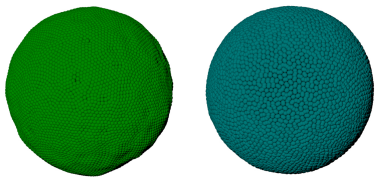

Figure 5: Comparison of the surface tension model by Becker and Teschner [BT07] with our modification of this model. With a surface tension coefficient of $\varphi = 0.08$ in combination with IISPH, the sphere is slightly deformed using their model (left). With our proposed modifications (right), an improved spherical shape is achieved.

placed on top of a dipping channel located above the glass. The choice of the surface tension model influences characteristics and form of the jet. Also, the fluid's behavior upon impact of the liquid on the inside of the glass depends on surface tension effects. Snapshots of the animations are shown in Fig. 10 and are discussed in Sec. 6.3. Here, we use the parameters $h = 0.1$ *m*, $\nu = 0.01$, and $dt = 0.001$ *s*.

6. Evaluation of Surface Tension Models Using Our Benchmark Tests

As mentioned before, we apply the tests of the previous section to the three surface tension models specified in Sec. 3.2 in combination with WCSPH, PCISPH, and IISPH respectively, resulting in up to 12 possible configurations. The used configurations and the corresponding parameters are given in the following sections.

Throughout this paper in images and plots, we color code the surface tension model by Akinci et al. [AAT13] with shades of red, the model of Becker and Teschner [BT07] with shades of green, the model of He et al. [HWZ*14] using shades of brown, and our modifications of the model of Becker and Teschner are represented in shades of blue.

6.1. Benchmark Test 1

We applied the benchmark test 1 as described in Sec. 5.1 to all nine configurations of SPH and surface tension models. Additionally, the simulations are conducted with five different parameters for the respective surface tension models (Sec. 3.2), resulting in 60 simulation runs. Unfortunately, the surface tension parameters for the different models have each a different physical meaning and hence, direct comparison is not possible. Therefore, we choose the parameter values equally spaced for each model, covering a range from low surface tension that slightly affects the shape of the fluid surface, to a very high value that has a major effect while achieving stable simulations. For both the model of Becker and Teschner [BT07] (Sec. 3.2.1) and our proposed modification (Sec. 3.2.4), we use the set of surface tension coefficients $\varphi = \{0.02, 0.035, 0.05, 0.065, 0.08\}$, for the model of Akinci et al. [AAT13] (Sec. 3.2.2), the used coefficients are $\gamma = \{0.2, 0.4, 0.6, 0.8, 1.0\}$, and for He et al. [HWZ*14] (Sec. 3.2.3), we use $\kappa = \{0.2, 0.6, 1.0, 1.4, 1.8\}$. We omit the respective units for the different coefficients, however we assume that length is given in *m* and time in *s*.

For a first visual inspection, snapshots of an example sequence are shown in Fig. 3. Full animations can be found in the accompanying video. Generally, as surface tension is applied, the particles move toward a spherical shape for all different models until an equilibrium state is reached. A comparison of the shapes of the equilibrium state with all models and surface tension coefficients can be found in the supplementary document. It has to be noted that the particles do not come to a rest state in this equilibrium, as surface tension forces work against pressure forces. Depending on the surface tension model and parameter value, particles slightly move around, but the overall shape of the fluid is maintained.

Using IISPH and PCISPH, a spherical shape is achieved with all models in most cases. Depending on the surface tension coefficient, the process is faster with higher values. However, using the model of He et al. [HWZ*14] with a low surface tension parameter, the surface tension forces are not large enough to sphere. As also discussed by Akinci et al. [AAT13], with the model of Becker and Teschner [BT07], particles tend to cluster as attracting forces are acting as particle move close to each other (see Fig. 2). In Fig. 5, we show that our modification to the model of Becker and Teschner (Sec. 3.2.4) alleviates particle clustering and improves the quality of the sphere. Moreover, it is possible to use higher surface tension coefficients compared to the original model while maintaining an undeformed spherical shape.

Another observation is that the different surface tension models have a different behavior regarding the convergence to the sphere shape. With the models of Becker and Teschner [BT07] and Akinci et al. [AAT13], the final shape of the equilibrium state is reached within a short period of time. It is noticeable that the drop oscillates in the first few frames with the model of Akinci et al., as opposed to the other models. In contrast, with the model of He et al. [HWZ*14], the process of drop formation takes considerably longer regarding simulation time.

The observed visual characteristics in the drop formation process can also be identified in measurements of particle velocities. Detailed velocity and force plots for all simulation runs can be found in the supplemental document. In all cases, the average velocity of the particles is converging to a certain value. Depending on the surface tension parameter, the equilibrium velocity is higher with a bigger parameter. For each model, velocities, as well as surface tension forces, scale almost linearly with the surface tension parameter in this test, as the plots in the supplemental document reveal. However, it has to be noted that this equilibrium velocity also depends on parameters of the underlying SPH simula-

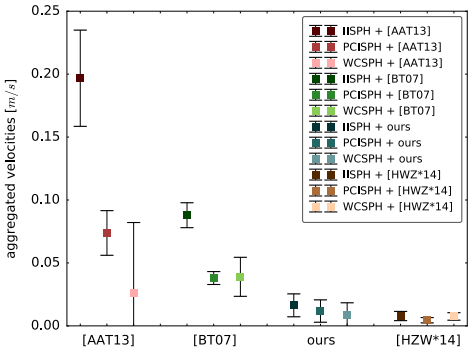

Figure 6: Aggregated average velocities with standard deviations for the simulations of benchmark test 1 with all configurations calculated using Eq. 13. For each surface tension model, aggregated velocities are shown in combination with each SPH model, which approximately correspond to the equilibrium velocities.

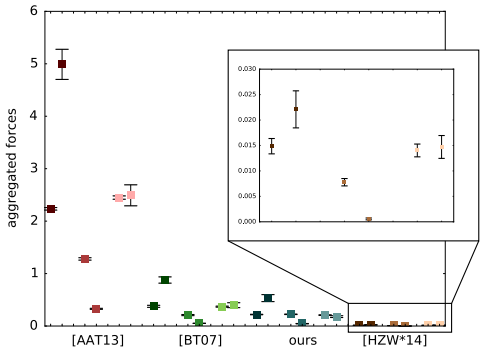

Figure 7: Aggregated forces in N with standard deviations for the simulations of benchmark test 1 with all configurations. For each combination of SPH method, aggregated surface tension forces F^{st} and pressure forces F^{p} are depicted in the same color, side by side. Left: surface tension model of Akinci et al. [AAT13] (red) with IISPH, PCISPH, and WCSPH. Center: similar, the models of Becker and Teschner [BT07] (green) and ours (blue). Right: the model of He et al. [HWZ*14] (brown).

tion, e.g. the smoothing length of the SPH kernel. For each combination of SPH and surface tension model, we calculate the aggregated values of the average velocities using

$$v^{aggr} = \sum_{i=1}^{N} \left(\sum_{j=0}^{M} |\mathbf{v}_j| / M \right) / N, \qquad (13)$$

where M is the number of frames and the $N = 5$ different surface tension coefficients. In Fig. 6, these aggregated values of the average velocities are shown. Regarding the different surface tension models, the method of Akinci et al. [AAT13] results in much higher velocities, whereas with the model of He et al. [HWZ*14], velocities are up to a factor of 100 lower and the process to a sphere takes much longer. With our modifications to the model of Becker and Teschner [BT07], lower end velocities are achieved.

Regarding varying SPH models, it can be observed that at least for the combination with the surface tension models using inter-particle forces, the resulting velocities are noticeably higher than with other solvers. Contrary to the IIF models, the method by He et al. [HWZ*14] is hardly influenced by the SPH method.

The oscillating sphere shape that can be observed in the animation of the combination of IISPH with the surface tension model of Akinci et al., appears as multiple local extreme values in the velocities (see temporal plot in supplemental document). In this case, four local maximum values can be identified. In comparison, the models of Becker and Teschner [BT07] and He et al. [HWZ*14] have only one local maximum that reflects that no oscillations occur.

In Fig. 7, aggregated surface tension forces and pressure forces, calculated similar to Eq. 13, are shown. As with other data, detailed force plots are provided in supplemental material. As expected, increasing surface tension parameter values results in higher surface tension forces, and the pressure forces that act opposite to the surface tension force, also increase. Comparing the different models, it is noticeable that the surface tension forces with the model of Akinci et al. are generally larger than with the other models (see Fig 7). Especially with the model of He et al. [HWZ*14], surface tension forces are considerably smaller, which explains the slower convergence of the particles velocities.

Another observation using WCSPH and PCISPH is that pressure forces are lower compared to IISPH. Especially with WCSPH, this prevents the sphere forming process with low surface tension coefficient.

6.2. Benchmark Test 2

The benchmark test 2 (Sec. 5.2) is applied to all surface tension models in combination with IISPH and WCSPH. As we aim to emphasize the main characteristics of the configurations, we use the lowest and the highest values in the sets of surface tension coefficients used for the first test, respectively. Therefore, 16 different simulation runs are analyzed.

In Fig. 8, snapshots of the liquid crown for the simulation models in combination with IISPH are shown. The shape of the crown differ considerably at the same frame using different simulation models. Especially with a high surface tension coefficient, the approach by Akinci et al. [AAT13] produces a smooth, flat crown shape where thin features are preserved. With the approach based on inter-particle interaction

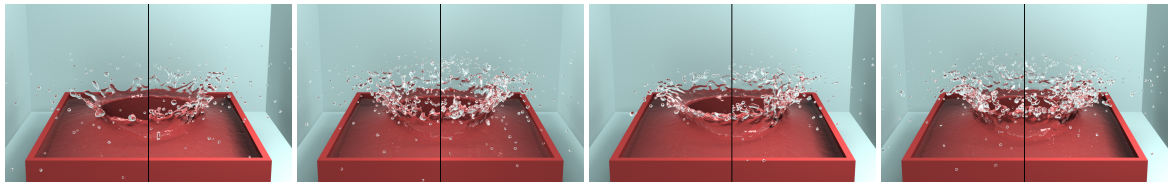

Figure 8: Snapshots of the animation as described in benchmark test 2 (Sec. 5.2) applied to different surface tension models in combination with IISPH. In each image, the largest surface coefficient is shown on the right side, the lowest on the left side. From left to right: the models of Akinci et al. [AAT13], Becker and Teschner [BT07], He et al. [HWZ*14], and our model.

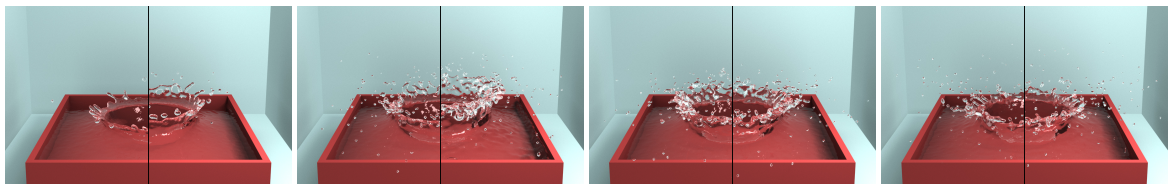

Figure 9: Snapshots of the animation as described in benchmark test 2 (Sec. 5.2) applied to different surface tension models in combination with WCSPH in the same order as in Fig. 8. With WCSPH, the height of the crown is lower and there are fewer droplets.

forces, the crown dissolves in many droplets and there are only minor differences visible between large and small surface tension coefficients. Shown on the right image of Fig. 8, the model by He et al. [HWZ*14] also leads to a smooth crown shape preserving thin features. As with all surface tension models, the height and slope of the crown increases with a lower surface tension coefficient. Using WCSPH (Fig. 9), similar effects can be observed. However, the shape of the crown is less extensive in all cases and fewer isolated particles exist at this frame. For the method of Becker and Teschner [BT07], differences between the surface tension coefficient are more obvious in the resulting animation.

Although there are considerable differences visually in the animations, the differences in average particle velocities between the small and the large surface tension coefficient are only marginal with all combinations and only differ slightly between the individual configurations. We refer to the supplemental document for temporal plots of the velocities. Generally, surface tension models smooth the velocities and high frequency oscillations disappear with an increased surface tension coefficient.

6.3. Benchmark Test 3

As surface tension effects become less prominent with larger free surface areas, we only evaluate the largest coefficients of the surface tension models in combination with IISPH to illustrate their impact in case of benchmark test 3 (Sec 5.3).

Again, snapshots of simulations using different surface tension models are shown for comparison in Fig. 10. As the liquid is poured into the glass, the shape of the liquid using the model by Akinci et al. [AAT13] differs substantially from the shapes resulting from the other models: a smooth continuous jet is formed, whereas with the other methods, many small droplets detach from the liquid jet. The animations created with the surface tension models of Becker and Teschner [BT07] and He et al. [HWZ*14] show only minor differences, mostly toward the end of the animation, when the liquid gradually stops pouring into the glass (see accompanying video). As in test 2, there are almost no noticeable differences in average particle velocities in this scenario.

6.4. Runtime Analysis

For runtime analysis, one second simulation time of the sequence of benchmark test 1 (Sec. 5.1) was simulated with the different classes of surface tension models combined with the IISPH model. All simulations were performed on a standard workstation with an Intel Core i7-3770 processor at 3.4 GHz and 32 GB RAM.

In Table 1, timings are given for the computation of surface tension forces, pressure forces, and overall forces computation. The calculation of surface tension forces is primarily coupled to the number of iterations over all particles that have to be performed. As only one iteration is needed for the surface tension model of Becker and Teschner [BT07], the fastest computation times for the evaluation of surface tension forces are achieved for these models. Our proposed modification described in Sec. 3.2.4 uses the same approach and no fundamental changes are necessary in the implementation, and therefore, similar runtimes are achieved. For the approach of Akinci et al. [AAT13], two iterations over all particles are necessary, which leads to higher computation times compared to Becker and Teschner. In our implementation, three iterations over all particles are necessary using

Figure 10: Liquid pouring into a glass using IISPH in combination with different surface tension models. Left: with the model of Akinci et al. [AAT13] ($\gamma = 1.0$), a smooth continuous jet of liquid is preserved, whereas with the models of Becker and Teschner [BT07] ($\varphi = 0.08$, center) and He et al. [HWZ*14] ($\kappa = 1.0$, right) many droplets emerge.

the model of He et al. [HWZ*14], as we use a separate iteration for the calculation of the color field (Eq. 10), resulting in the highest computation times.

Besides differences between the individual surface tension models, there is no noticeable impact of the value of the surface tension coefficent on the performance of a model. Also, for all simulation models, we observe only low deviations in the calculation of the pressure force calculation.

7. Discussion

After performing tests on different surface tension models across different SPH implementations, it can be observed that the surface tension models have considerably varying characteristics. These differences not only affect the visual results, but also the physical quantities of the simulations. In addition, the underlying SPH implementation in combination with the surface tension model, affects the overall behavior of the simulation and leads to a wide range of factors steering the outcome of the animation. The manifold influences have to be considered for producing artistically controlled simulations bearing a desired look and have a major effect on the process of developing surface tension models.

From Sec. 6.1, it can be seen that the convergence behavior in the process of the drop formation varies greatly for the tested surface tension models. Despite the fact that all of the models generate a spherical shape of the drop with an appropriate surface tension coefficient, the speed and temporal behavior is different. On the one hand, the absolute value of the surface tension force affects the threshold when the final shape is reached. With large surface tension forces exhibited by the models of Becker and Teschner [BT07] and Akinci et al. [AAT13], it occurs much earlier than with the noticeably smaller surface tension forces of the model by He et al. [HWZ*14]. On the other hand, smaller forces lead to a much steadier equilibrium state. These smaller forces, however, do not offer the possibility of an oscillating drop as

Table 1: Timings in *s* for a one second simulation time of the benchmark test 1 (drop formation) using the different surface tension (ST) models combined with IISPH. Runtimes are given for the calculation of surface tension forces $\mathbf{F}^{st}$, pressure forces $\mathbf{F}^{p}$, and overall force computation $\mathbf{F}^{t}$.

ST model	ST coeff.	$\mathbf{F}^{st}$	$\mathbf{F}^{p}$	$\mathbf{F}^{t}$
[AAT13]	$\gamma = 0.2$	26.89	97.48	310.00
[AAT13]	$\gamma = 1.0$	26.49	106.30	313.00
[BT07]	$\varphi = 0.02$	16.80	98.32	307.10
[BT07]	$\varphi = 0.08$	16.23	93.76	298.23
[HWZ*14]	$\kappa = 0.2$	54.79	88.19	329.73
[HWZ*14]	$\kappa = 1.8$	52.82	95.48	339.83

produced by the model of Akinci et al. with a large surface tension coefficient, which rather coincides with the observed physical behavior of a real water drop in absence of gravity.

Especially with the surface tension models by Akinci et al. [AAT13] and Becker and Teschner [BT07], a dissipative effect when using WCSPH is perceivable. The lower pressure forces that counteract surface tension forces lead to lower velocities in comparison with IISPH and PCISPH, as it can be observed in benchmark test 1. We expect this effect to be more distinct when using a lower EOS constant.

There is a large space of possible animations that not only depends on a parameter, but on the interplay of simulation and surface tension models. The different approaches to surface tension (Sec. 3.2) reveal considerable differences. Hence, from a production point of view, the choice of a surface tension model and the corresponding coefficient strongly depends on the objective:

- Should animations exhibit a behavior that recreates effects observable in reality, such as the oscillation of a drop, the model of Akinci et al. [AAT13] is especially suitable.
- Should thin features be preserved in combination with smooth surfaces, the model of He et al. [HWZ*14] produces pleasing results as well.
- For a compromise between computational efficiency and plausible surface tension effects at a small scale, the method of Becker and Teschner [BT07], especially with our proposed modification, is a good candidate.

We also believe that the proposed testing environment not only helps regarding the comparability of surface tension models, but represents a useful set of tests that can be used in the development of new surface tension models. Using the benchmark, new models can be directly compared to existing approaches and several properties appear immediately.

8. Conclusions

We presented a systematic evaluation of surface tension models for SPH-based fluid animations. To this end, a benchmark test consisting of three scenarios and selected

measurements has been proposed. The uniform setup of our tests not only allow a consistent and reproducible comparison of surface tension models, but it is also suitable to identify the specific characteristics of these models, in particular in combination with varying SPH approaches. Besides a visual comparison on a standardized basis, our proposed measurements allow for quantitative analysis for the examination of configurations from an animation point of view.

We applied the tests to three types of surface tension models in combination with three different SPH techniques. Using our uniform specifications, we identified some of the specific properties of surface tension models in a comparative manner. It is also possible to apply our benchmark to newly developed algorithms to be able to see the performance compared to existing methods. Further, we proposed a simple modification to the surface tension model of Becker and Teschner [BT07] to improve the quality of results with the same simplicity.

By providing source code to the benchmarks, researchers will be able to compare their algorithms to our findings.

As future work, we plan to further improve our modification to the surface tension model by Becker and Teschner [BT07] (Sec. 3.2.4). Further, it could be interesting to incorporate models that include the air phase in the modeling of surface tension models, e.g. using ghost particles [SB12] or multi-fluid models [MSKG05], [SP08]. Also, extending benchmark to related effects, such as adhesion and capillarity would be a promising research direction. Generally, the development and application of benchmark tests to other areas of fluid animation is an interesting topic.

Acknowledgements

This work was partly supported by "Kooperatives Promotionskolleg Digital Media" at Stuttgart Media University and the University of Stuttgart.

References

[AAIT12] AKINCI G., AKINCI N., IHMSEN M., TESCHNER M.: An efficient surface reconstruction pipeline for particle-based fluids. In *Workshop on Virtual Reality Interaction and Physical Simulation* (2012), pp. 61–68. 2

[AAT13] AKINCI N., AKINCI G., TESCHNER M.: Versatile surface tension and adhesion for SPH fluids. *ACM Transactions on Graphics 32*, 6 (2013), 182:1–182:8. 2, 4, 5, 6, 7, 8, 9

[AIA*12] AKINCI N., IHMSEN M., AKINCI G., SOLENTHALER B., TESCHNER M.: Versatile rigid-fluid coupling for incompressible SPH. *ACM Transactions on Graphics 31*, 4 (2012), 62:1–62:8. 5

[APKG07] ADAMS B., PAULY M., KEISER R., GUIBAS L. J.: Adaptively sampled particle fluids. *ACM Transactions on Graphics 26*, 3 (2007). 2

[BGB15] BHATTACHARYA H., GAO Y., BARGTEIL A. W.: A level-set method for skinning animated particle data. *IEEE Transactions on Visualization and Computer Graphics 21*, 3 (2015), 315–327. 2, 3, 5

[BKZ92] BRACKBILL J. U., KOTHE D. B., ZEMACH C.: A continuum method for modeling surface tension. *Journal of Computational Physics 100*, 2 (1992), 335–354. 4

[BT07] BECKER M., TESCHNER M.: Weakly compressible SPH for free surface flows. In *ACM SIGGRAPH/Eurographics Symposium on Computer Animation* (2007), pp. 209–218. 2, 3, 4, 5, 6, 7, 8, 9, 10

[EFFM02] ENRIGHT D., FEDKIW R., FERZIGER J., MITCHELL I.: A hybrid particle level set method for improved interface capturing. *Journal of Computational Physics 183*, 1 (2002), 83–116. 2

[HEW15] HUBER M., EBERHARDT B., WEISKOPF D.: Boundary handling at cloth–fluid contact. *Computer Graphics Forum 34*, 1 (2015), 14–25. 3

[HWZ*14] HE X., WANG H., ZHANG F., WANG H., WANG G., ZHOU K.: Robust simulation of sparsely sampled thin features in SPH-based free surface flows. *ACM Transactions on Graphics 34*, 1 (2014), 7:1–7:9. 2, 4, 6, 7, 8, 9

[ICS*14] IHMSEN M., CORNELIS J., SOLENTHALER B., HORVATH C., TESCHNER M.: Implicit incompressible SPH. *IEEE Transactions on Visualization and Computer Graphics 20*, 3 (2014), 426–435. 3

[IOS*14] IHMSEN M., ORTHMANN J., SOLENTHALER B., KOLB A., TESCHNER M.: SPH fluids in computer graphics. In *EG 2014 - STARs* (2014), pp. 21–42. 2, 3, 5

[MCG03] MÜLLER M., CHARYPAR D., GROSS M.: Particle-based fluid simulation for interactive applications. In *ACM SIGGRAPH/Eurographics Symposium on Computer Animation* (2003), pp. 154–159. 2, 4, 5

[MFZ97] MORRIS J. P., FOX P. J., ZHU Y.: Modeling low Reynolds number incompressible flows using SPH. *Journal of Computational Physics 136*, 1 (1997), 214–226. 5

[Mon05] MONAGHAN J. J.: Smoothed particle hydrodynamics. *Reports on Progress in Physics 68*, 8 (2005), 1703–1759. 5

[Mor00] MORRIS J. P.: Simulating surface tension with smoothed particle hydrodynamics. *International Journal for Numerical Methods in Fluids 33*, 3 (2000), 333–353. 4

[MSKG05] MÜLLER M., SOLENTHALER B., KEISER R., GROSS M.: Particle-based fluid-fluid interaction. In *ACM SIGGRAPH/Eurographics Symposium on Computer Animation* (2005), pp. 237–244. 10

[SB12] SCHECHTER H., BRIDSON R.: Ghost SPH for animating water. *ACM Transactions on Graphics 31*, 4 (2012), 61:1–61:8. 10

[SP08] SOLENTHALER B., PAJAROLA R.: Density contrast SPH interfaces. In *ACM SIGGRAPH/Eurographics Symposium on Computer Animation* (2008), pp. 211–218. 10

[SP09] SOLENTHALER B., PAJAROLA R.: Predictive-corrective incompressible SPH. *ACM Transactions on Graphics 28*, 3 (2009), 40:1–40:6. 3

[SSP07] SOLENTHALER B., SCHLÄFLI J., PAJAROLA R.: A unified particle model for fluid–solid interactions. *Computer Animation and Virtual Worlds 18*, 1 (2007), 69–82. 2

[TM05] TARTAKOVSKY A., MEAKIN P.: Modeling of surface tension and contact angles with smoothed particle hydrodynamics. *Physical Review E 72* (2005), 026301. 3, 4

[YT13] YU J., TURK G.: Reconstructing surfaces of particle-based fluids using anisotropic kernels. *ACM Transactions on Graphics 32*, 1 (2013), 5:1–5:12. 3

[ZB05] ZHU Y., BRIDSON R.: Animating sand as a fluid. *ACM Transactions on Graphics 24*, 3 (2005), 965–972. 2, 3